

How to detect GeV neutrinos
using a magnetised detector?
Iron Calorimeter @
India-based Neutrino Observatory

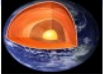
Lakshmi.S.Mohan

FUW High Energy Physics Seminar
28-01-2022

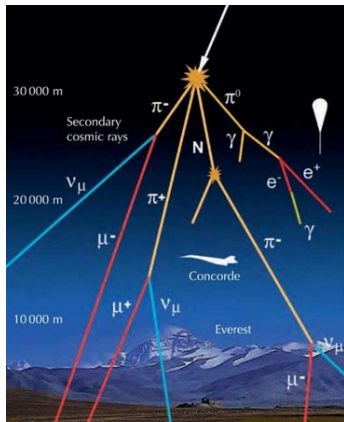
Contents

- Atmospheric neutrinos and their oscillations
- Earth matter effects
- ICAL@INO
- Detector R&D
- Simulation studies
- Estimated sensitivities to 2-3 oscillation parameters
- Current status: mini-ICAL

Neutrinos from different sources can be studied

Source	Energy	Facts
Big bang relic ν 	$1.95 \text{ K} \sim 2 \times 10^{-4} \text{ eV}$	2 nd most abundant particle in the universe ($\sim 330 \text{ cm}^{-3}$)
Earth (Geo ν) 	$< 3 \text{ MeV}$	$\bar{\nu}_e$ from β decay of natural isotopes like ^{238}U , ^{232}Th , ^{40}K
Reactors 	$\sim 3 \text{ MeV}$	ν_e from β decay of fission products in a nuclear reactor (Reines and Cowan)
Sun 	a few MeV	Fusion in pp chain or CNO cycle Flux @ Earth's surface : $6 \times 10^{10} \text{ cm}^{-2} \text{ s}^{-1}$ @ $E_\nu \leq 0.42 \text{ MeV}$; $5 \times 10^6 \text{ cm}^{-2} \text{ s}^{-1}$ @ $0.8 \text{ MeV} \leq E_\nu \leq 15 \text{ MeV}$
Supernovae 	10-30 MeV	Supernova explosion (ex.) SN1987A
Earth's atmosphere 	0.1 MeV - 1000 GeV	Decay of pions and kaons in cosmic rays
Particle accelerators 	a few GeVs	Decay of pions and kaons produced in a lab
(Extra-)Galactic sources 	TeV - PeV	astrophysical sources

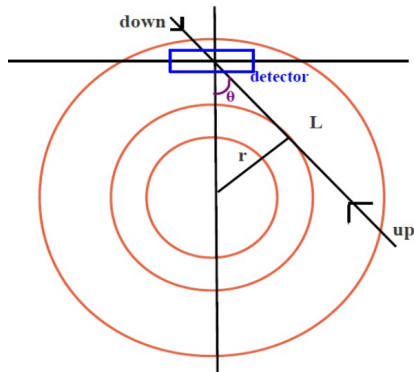
Production of atmospheric neutrinos



$$\pi^\pm \rightarrow \mu^\pm + \nu_\mu(\bar{\nu}_\mu);$$

$$\mu^\pm \rightarrow e^\pm + \bar{\nu}_\mu(\nu_\mu) + \nu_e(\bar{\nu}_e),$$

$$R = \frac{(\Phi_{\nu_\mu} + \Phi_{\bar{\nu}_\mu})}{(\Phi_{\nu_e} + \Phi_{\bar{\nu}_e})} \approx 2$$



- Span a wide range of L/E
 L = distance traversed by the neutrino, ~ 15 km – ~ 12700 km
 E = its energy in GeV
- Detection via charged current and neutral current interaction in a detector

India and atmospheric neutrinos - Throwback

Discovery of atmospheric neutrinos (1965)

In 1965, atmospheric neutrinos were observed for the first time by detectors located very deep underground.

← In South Africa

F. Reines et al., PRL 15, 429 (1965)

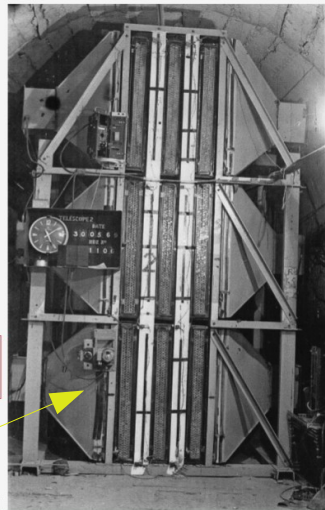
→ In India

C.V. Achar et al., PL 18, 196 (1965)

**Kolar Gold Field
(KGF) experiment**

Photo by H.Sbel

Photo by N. Mondal



Earth matter effects on neutrino oscillations

- What we detect at the detector are the *flavour eigen states*
- i.e. ν_e, ν_μ, ν_τ .
- Flavour states are superimpositions of mass eigen states
 $\nu_i, i = 1, 2, 3; |\nu_\alpha\rangle = \sum_i U_{\alpha i} |\nu_i\rangle, \alpha = e, \mu, \tau, i = 1, 2, 3.$

$$U_{\alpha i}^{vac} = \begin{pmatrix} c_{12}c_{13} & s_{12}c_{13} & s_{13}e^{-i\delta} \\ -c_{23}s_{12} - s_{23}c_{12}s_{13}e^{i\delta} & c_{23}c_{12} - s_{23}s_{12}s_{13}e^{i\delta} & s_{23}c_{13} \\ s_{23}s_{12} - c_{23}c_{12}s_{13}e^{i\delta} & -s_{23}c_{12} - c_{23}s_{12}s_{13}e^{i\delta} & c_{23}c_{13} \end{pmatrix},$$

where, $c_{ij} = \cos \theta_{ij}$ and $s_{ij} = \sin \theta_{ij}; i, j \rightarrow$ mass eigenstates.

θ_{ij} – mixing angles, δ_{CP} leptonic CP violation phase

Oscillation probability in vacuum

- Mass eigen states evolve in time : $|\nu_i(t)\rangle = e^{-iE_it}|\nu_i(0)\rangle$
- Consequently flavor eigen states also evolve in time :
$$|\nu_\alpha(t)\rangle = \sum_{\beta=e,\mu,\tau} \left(\sum_i U_{\alpha i} e^{-iE_it} U_{\beta i}^* \right) |\nu_\beta\rangle$$

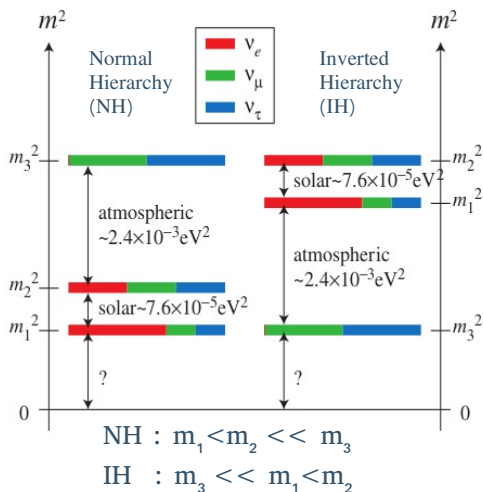
Probability of a neutrino flavour $|\nu_\alpha\rangle$ ($|\bar{\nu}_\alpha\rangle$) of energy E oscillating to another flavour $|\nu_\beta\rangle$ ($|\bar{\nu}_\beta\rangle$) after travelling a distance L :

$$\begin{aligned} P_{\alpha\beta}^{(-)} &= \delta_{\alpha\beta} - 4 \sum_{i>j} \text{Re} [U_{\alpha i} U_{\beta i}^* U_{\alpha j}^* U_{\beta j}] \sin^2 \left(\frac{\Delta m_{ij}^2 L}{4E} \right) \\ &\pm 2 \sum_{i>j} \text{Im} [U_{\alpha i} U_{\beta i}^* U_{\alpha j}^* U_{\beta j}] \sin \left(\frac{\Delta m_{ij}^2 L}{2E} \right). \end{aligned}$$

Current status of neutrino oscillation parameters

- **Known:** $\theta_{12} \approx 33.45^\circ$, $\theta_{13} \approx 8.6^\circ$, $\Delta m_{21}^2 = 7.42 \times 10^{-5} \text{ eV}^2$
- **Being measured:** $\theta_{23} \approx 45.55^\circ$, $|\Delta m_{31}^2| = 2.5 \times 10^{-3} \text{ eV}^2$
- **Unknown:** Sign of Δm_{32}^2 (mass hierarchy) & δ_{CP}

The question of mass hierarchy



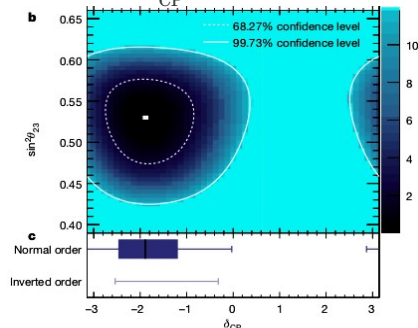
Octant of $\theta_{23} = ?$

$\theta_{23} < 45^\circ$: Lower octant

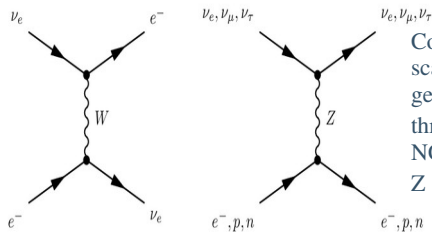
$\theta_{23} = 45^\circ$: Maximal

$\theta_{23} > 45^\circ$: Higher octant

Hints of $\delta_{CP} \approx -90^\circ$ from T2K



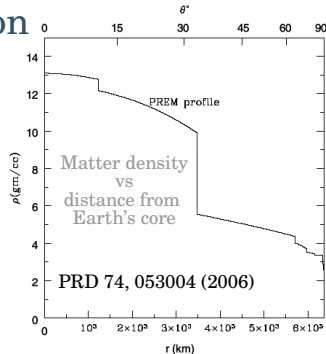
Earth matter effects on neutrino propagation



Coherent forward elastic scattering processes generate CC potential V_{CC} through W exchange and NC potential V_{NC} through Z exchange.

$$A_{CC} = 2EV_{CC} = 2\sqrt{2}G_F n_e E = 7.63 \times 10^{-5} \rho(\text{gm/cc}) E(\text{GeV}) \text{eV}^2,$$

G_F = Fermi constant; n_e = electron number density in matter; ρ = the matter density



Resonance in Earth matter

Non-zero θ_{13} is crucial

$$\sin 2\theta_{13}^m = \frac{\sin 2\theta_{13}}{[(\cos 2\theta_{13} - (A_{CC}/\Delta m_{32}^2))^2 + \sin^2 2\theta_{13}]^{1/2}}$$

Resonance condition: $\cos 2\theta_{13} = A_{CC}/\Delta m_{32}^2$

Occurs in $\nu(\bar{\nu})$ if the true hierarchy is **normal** (inverted).

Matter effects affect the time evolution of flavour states

$$i\frac{d\tilde{\nu}}{dt} = \frac{1}{2E} [UM^2U^\dagger + A] \tilde{\nu} \quad E = \text{Neutrino energy}$$

$$M^2 = \text{diag}(m_1^2, m_2^2, m_3^2)$$

$$A = \begin{pmatrix} A_{CC} & 0 & 0 \\ 0 & 0 & 0 \\ 0 & 0 & 0 \end{pmatrix} \text{ and } \tilde{\nu} = (\nu_e, \nu_\mu, \nu_\tau)^T$$

A_{CC} is +ve for ν and -ve for anti- ν

P_{osc} & \bar{P}_{osc} are modified differently according to the sign of Δm_{31}^2 .

Oscillation channels of interest in atmospheric neutrinos

- $\nu_\mu \rightarrow \nu_\alpha ; \bar{\nu}_\alpha \rightarrow \bar{\nu}_\mu$
- $\nu_e \rightarrow \nu_\alpha ; \bar{\nu}_e \rightarrow \bar{\nu}_\alpha$
- $\alpha = e, \mu, \tau$

Oscillograms generated with:

$$\theta_{12} = 33.45^\circ,$$

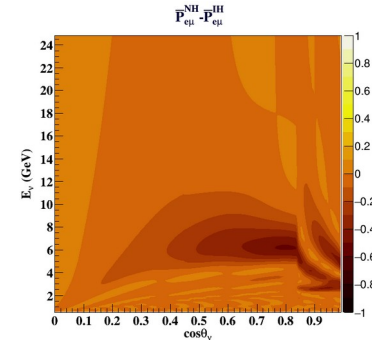
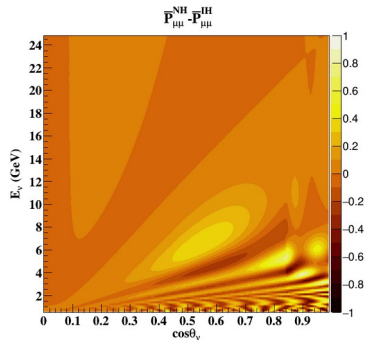
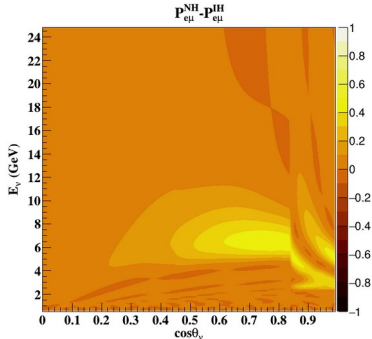
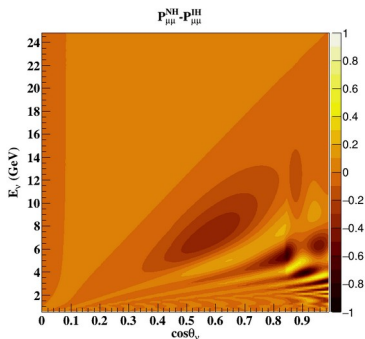
$$\Delta m_{21}^2 = 7.42 \times 10^{-5} \text{ eV}^2$$

$$\theta_{13} = 8.6^\circ,$$

$$\theta_{23} = 45^\circ,$$

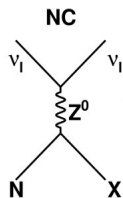
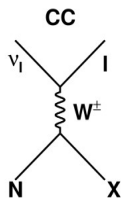
$$|\Delta m_{\text{eff}}^2| = 2.52 \times 10^{-3} \text{ eV}^2$$

$$\delta_{\text{CP}} = 0^\circ$$



Motivation for a magnetized neutrino detector

- A detector capable of probing the resonance region can determine mass hierarchy.
- Detectors that can identify ν and $\bar{\nu}$ separately can determine hierarchy and confirm that resonance is indeed happening. → Identify the charge of the final lepton from a charged current (CC) interaction with target.



$$l = e, \mu, \tau$$

$\nu_l =$ neutrino of flavour l

$N =$ target nucleon

$$\nu_l + N \rightarrow l^- + X$$

$$\nu_l + N \rightarrow \nu_l + X$$

$$\bar{\nu}_l + N \rightarrow l^+ + X$$

$$\bar{\nu}_l + N \rightarrow \bar{\nu}_l + X$$

Main oscillation channels of interest:

$$\nu_\mu \rightarrow \nu_\mu ; \bar{\nu}_\mu \rightarrow \bar{\nu}_\mu$$

$$\nu_e \rightarrow \nu_\mu ; \bar{\nu}_e \rightarrow \bar{\nu}_\mu$$

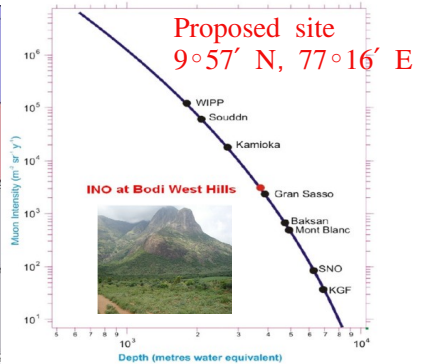
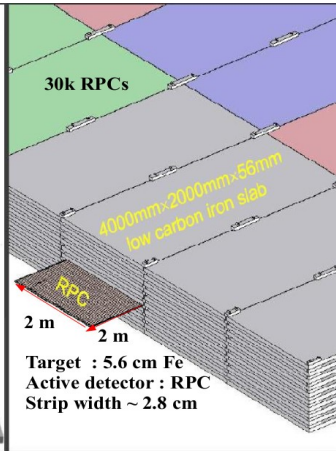
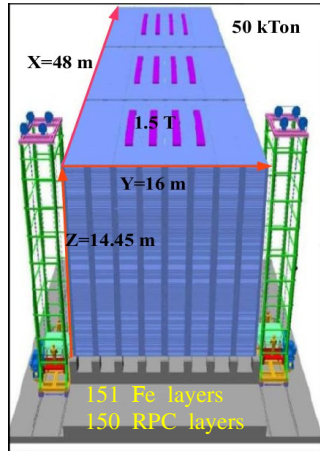
Magnetize a detector optimized for GeV μ^- , μ^+ detection → Enables charge identification (CID)

For $l = \mu$, **long track** in the detector.

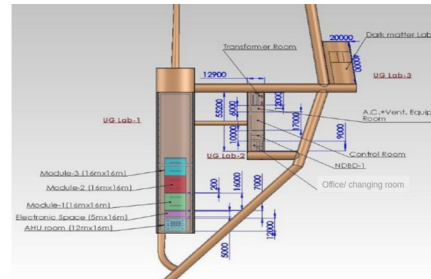
μ^- & μ^+ separation by magnetic field.

ICAL!

Iron CALorimeter (ICAL) @ India-based Neutrino Observatory (INO)



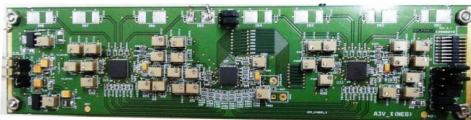
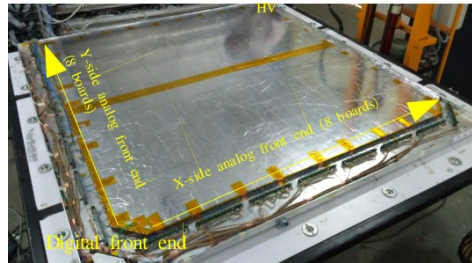
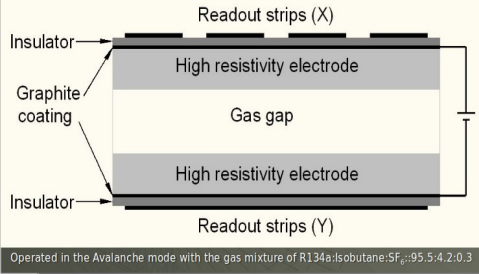
- Main experiment – ICAL
- Will also house a neutrinoless double beta decay (NDBD) experiment TINTIN in a nearby experimental hall.



Components of ICAL detector

- Target material – 5.6 cm Fe plates
- Active detectors for charged particle detection – Resistive Plate Chambers (RPCs)

➤ Two modes of operation possible
Avalanche and streamer modes

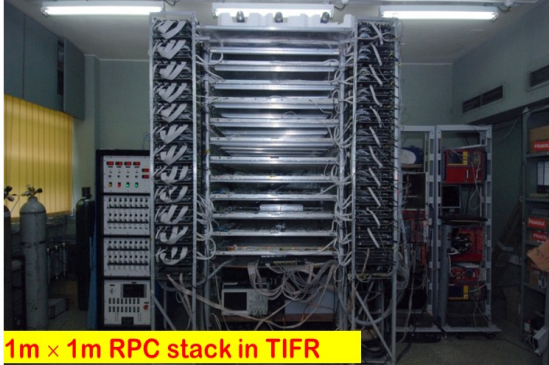


Anusparsh RPC AFE developed in BARC



RPCDAQ board
for RPC DFE

For a detailed talk on INO electronics:
<https://www.youtube.com/watch?v=hA4ywCdNjhA>



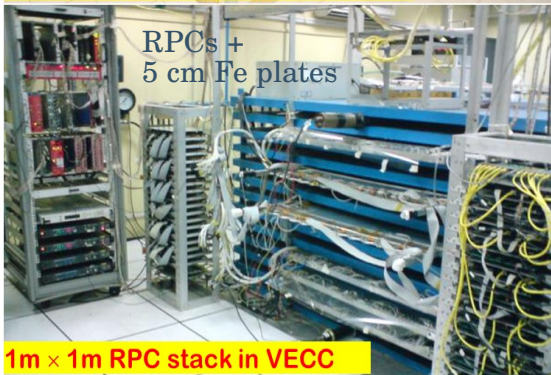
1m × 1m RPC stack in TIFR



2m × 2m RPC test stand in TIFR



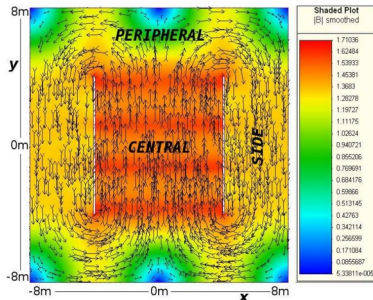
2m × 2m RPC stack in Madurai



RPCs +
5 cm Fe plates

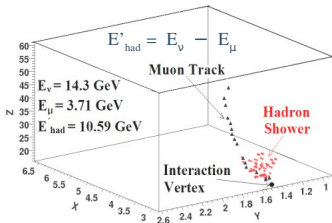
1m × 1m RPC stack in VECC

Detector simulation – resolutions and efficiencies



Magnetic field map simulated using MAGNET6.26 in a single iron plate at $z = 0$ Of ICAL detector.

A $CC\nu_{\mu}$ interaction in ICAL



NUANCE

Neutrino Event Generation



Generates particles that result from a random interaction of a neutrino with matter using theoretical models for both neutrino fluxes and cross-sections.

Output:

- Reaction Channel
- Vertex and time information
- Energy and momentum of all final state particles

GEANT4

Event Simulation

$\ell + X$ through simulated ICAL. Simulates propagation of particles through the ICAL detector with RPCs and magnetic field.

Output:

- x, y, z, t of the particles as they propagate through detector
- Energy deposited
- Momentum information

DIGITISATION

Event Digitisation

(X, Y, Z, T) of final states on including noise and detector efficiency

Output:

- Digitised output of the previous stage

Add detector efficiency and noise to the hits.

ANALYSIS

Event Reconstruction

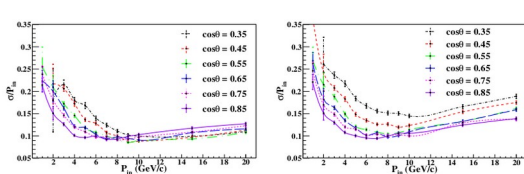
(E, \vec{p}) of ℓ, X (total hadrons)
Fit the muon tracks using Kalman filter techniques to reconstruct muon energy and momentum; use hits in hadron shower to reconstruct hadron information.

Output:

- Energy and momentum of muons and hadrons, for use in physics analyses.

Momentum and direction resolutions of muons with $p_\mu = 1\text{-}20$ GeV/c

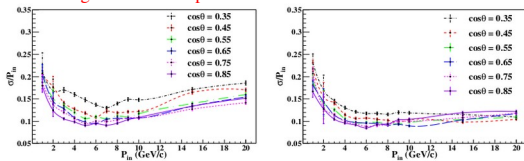
Muons in ICAL are reconstructed using Kalman filter algorithm



(a) $|\phi| \leq \pi/4$.

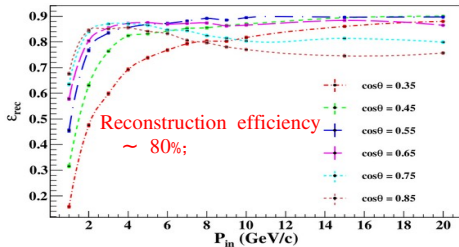
(b) $\pi/4 < |\phi| \leq \pi/2$.

Average direction-dependent momentum resolution $\sim 9\text{-}14\%$

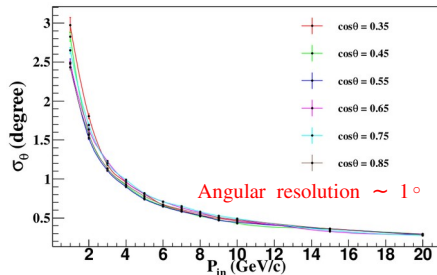


(c) $\pi/2 < |\phi| \leq 3\pi/4$.

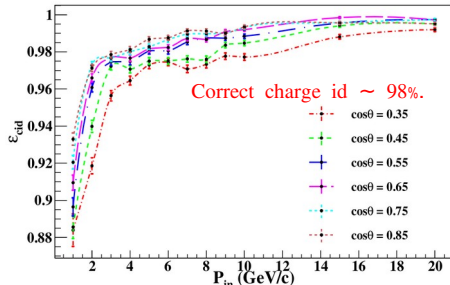
(d) $3\pi/4 < |\phi| \leq \pi$.



Reconstruction efficiency $\sim 80\%$;



Angular resolution $\sim 1^\circ$



Correct charge id $\sim 98\%$.

Hadrons in ICAL

- ~ 80% of hadrons → pions
- No information of charge deposited, so no calorimetric way to determine hadron energy.
- Energy calibrated to total number of hits in the hadron shower.

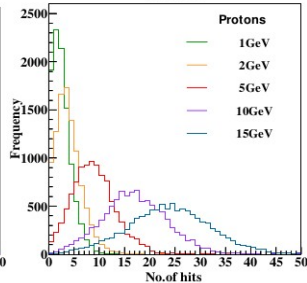
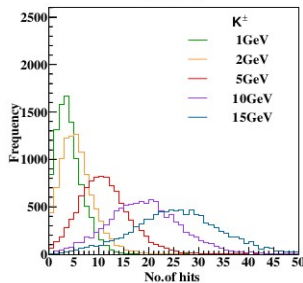
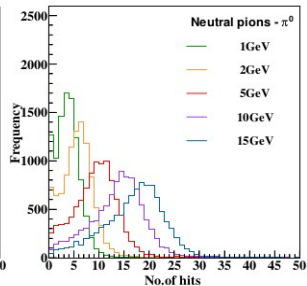
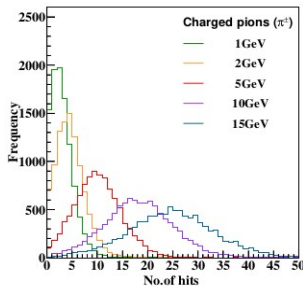
Only “hit” information is available for hadrons.
Number of hits → energy resolution.
Position & timing of hits → direction resolution.

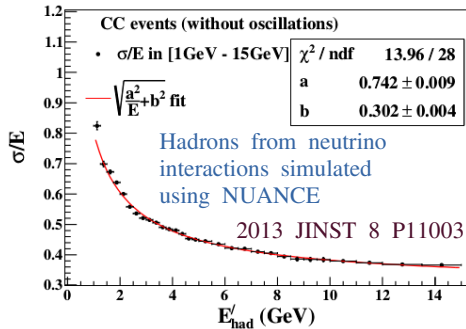
Mean number of hits:
 $\bar{n}(E) = n_0[1 - \exp(-E/E_0)]$,
where n_0 and E_0 are constants.

$E_0 \gg E$ for $E \leq 15$ GeV.

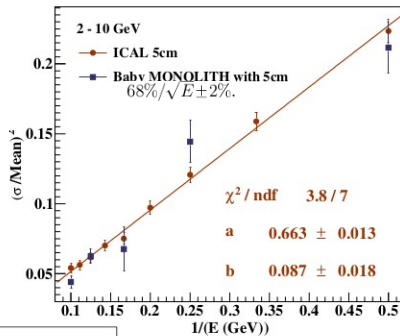
$$\frac{\bar{n}(E)}{n_0} = \frac{E}{E_0}$$

$$\frac{\sigma}{E} = \frac{\Delta n(E)}{\bar{n}(E)}$$

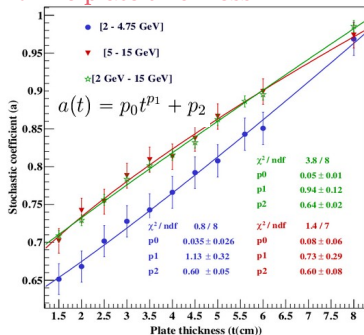
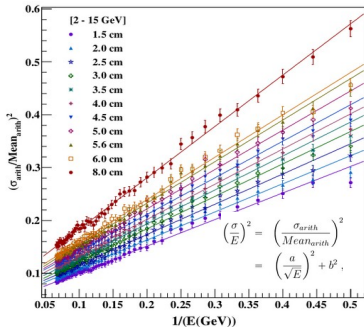




Comparison of ICAL simulation with Baby Monolith test beam data

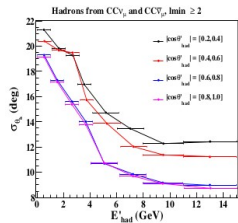
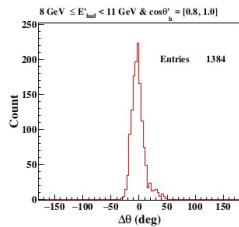
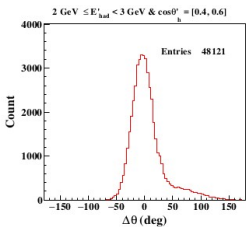


Dependence of energy resolution on Fe plate thickness



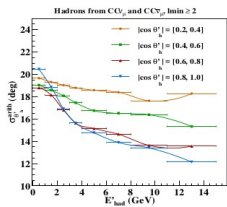
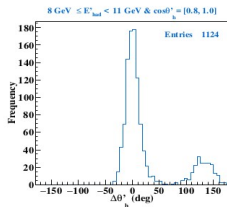
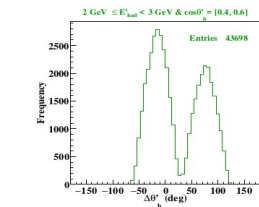
2014 JINST 9 T09003

Hadron direction resolution



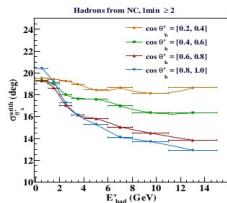
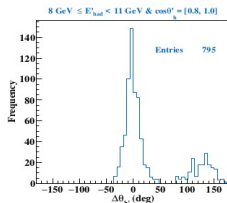
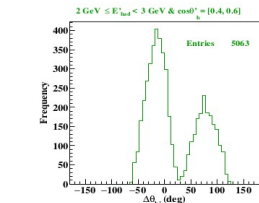
Orientation matrix method (OMM)

- Needs vertex information



Raw hit method (RHM)

- Does not need vertex information



Sensitivities to neutrino oscillation parameters in the 2–3 sector – simulation studies

No. of charged current muon neutrino events detected in ICAL:

$$\frac{d^2 N}{dE_\mu d \cos \theta_\mu} = t \times n_d \times \int dE_\nu d \cos \theta_\nu d\phi_\nu \times \left[P^{\mu\mu}_m \frac{d^3 \Phi_\mu}{dE_\nu d \cos \theta_\nu d\phi_\nu} + P^{e\mu}_m \frac{d^3 \Phi_e}{dE_\nu d \cos \theta_\nu d\phi_\nu} \right] \times \frac{d\sigma_\mu(E_\nu)}{dE_\mu d \cos \theta_\mu} \quad (3)$$

where,

- t = exposure time
- n_d = number of target nucleons in the detector
- σ_μ = the differential neutrino interaction cross section in terms of the energy and direction of the CC lepton produced
- Φ_μ and $\Phi_e \rightarrow \nu_\mu$ and ν_e fluxes
- $P^m_{\alpha\beta}$ = oscillation probability of $\nu_\alpha \rightarrow \nu_\beta$ in matter 11
- α, β different flavours.

Similarly for anti-neutrinos.

$$\chi_{\pm}^2 = \min_{\xi_l^{\pm}} \sum_{i=1}^{N_{E_{\mu}^{obs}}} \sum_{j=1}^{N_{\cos \theta_{\mu}^{obs}}} \left(\sum_{k=1}^{N_{E_{had}^{obs}}} \right) 2 \left[\left(T_{ij(k)}^{\pm} - D_{ij(k)}^{\pm} \right) - D_{ij(k)}^{\pm} \ln \left(\frac{T_{ij(k)}^{\pm}}{D_{ij(k)}^{\pm}} \right) \right] + \sum_{l^{\pm}=1}^5 \xi_{l^{\pm}}^2,$$

$$\chi_{10}^2 = \chi_{+}^2 + \chi_{-}^2$$

$$\chi_{\text{prior}}^2 = \left(\frac{\sin^2 2\theta_{13} - \sin^2 2\theta_{13}^{\text{true}}}{\sigma(\sin^2 2\theta_{13})} \right)^2$$

$$\chi_{\text{ICAL}}^2 = \chi_{10}^2 + \chi_{\text{prior}}^2,$$

$$T_{ij(k)}^{\pm} = T_{ij(k)}^{0\pm} \left(1 + \sum_{l^{\pm}=1}^5 \pi_{ij(k)}^{l^{\pm}} \xi_{l^{\pm}} \right)$$

$\pi_1 = 20\%$ flux normalisation error,

$\pi_2 = 10\%$ cross section error,

$\pi_3 = 5\%$ tilt error,

$\pi_4 = 5\%$ zenith angle error,

$\pi_5 = 5\%$ overall systematics.

- Marginalised over 3σ ranges of θ_{23} , Δm_{32}^2 and θ_{13}

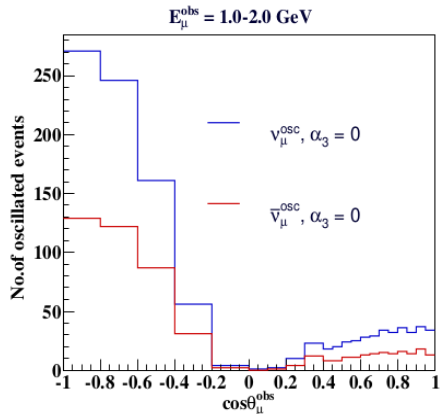
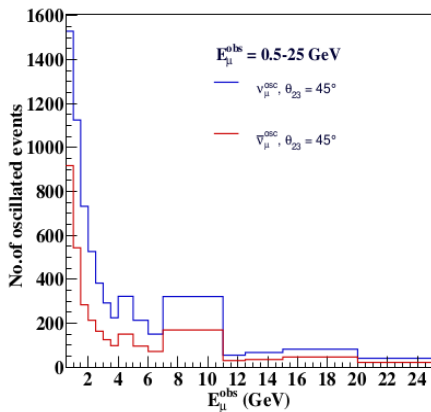
Parameter	True value	Marginalization range
θ_{13}	8.729°	$[7.671^{\circ}, 9.685^{\circ}]$
$\sin^2 \theta_{23}$	0.5	$[0.36, 0.66]$
Δm_{32}^2	$2.4 \times 10^{-3} \text{ eV}^2$	$[2.1, 2.6] \times 10^{-3} \text{ eV}^2$ (NH)
$\sin^2 \theta_{12}$	0.304	Not marginalised
Δm_{21}^2	$7.6 \times 10^{-5} \text{ eV}^2$	Not marginalised
δ_{CP}	0°	Not marginalised

Binning schemes

- 1 $(E_{\mu}^{obs}, \cos \theta_{\mu}^{obs})$ only, in E_{μ}^{obs} in $[0.5 - 25 \text{ GeV}]$, $\cos \theta_{\mu}^{obs}$ in $[-1, 1]$.
- 2 $(E_{\mu}^{obs}, \cos \theta_{\mu}^{obs}, E_{had}^{obs})$ with E_{μ}^{obs} in $[0.5 - 25 \text{ GeV}]$, $\cos \theta_{\mu}^{obs}$ in $[-1, 1]$ and E_{had}^{obs} in $[0 - 15 \text{ GeV}]$.

LSM thesis

Event spectra after applying oscillations

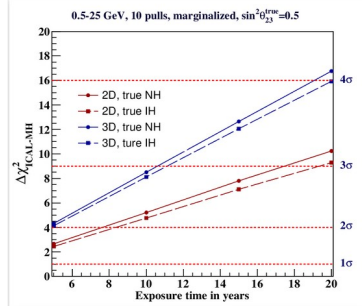
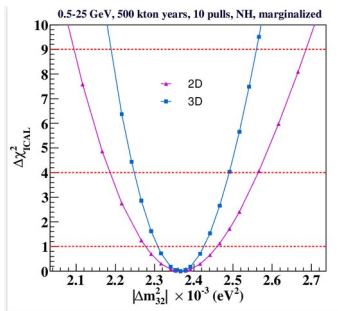
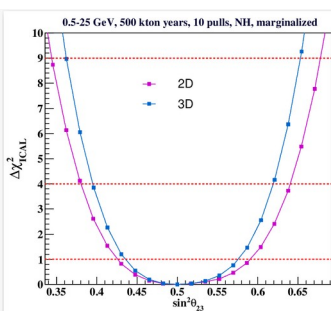


15 E_{μ}^{obs} bins, 21 $\cos\theta_{\mu}^{obs}$ and 4 E'_h bins.

μ only analysis (2D) : $(E_{\mu}^{obs}, \cos\theta_{\mu}^{obs})$: $15 \times 21 = 315$ bins

With hadron analysis (3D) : $(E_{\mu}^{obs}, \cos\theta_{\mu}^{obs}, E'_{obs_{had}})$:

$15 \times 21 \times 4 = 1260$ bins; 0.01 events expected per bin.



Relative 1σ precision: $p(\lambda) = \frac{\lambda_{\text{max}-2\sigma} - \lambda_{\text{min}-2\sigma}}{4\lambda_{\text{true}}}$

Parameter	Binning	Relative 1σ Precision (%) for true NH & 500 kton year exposure
$\sin^2\theta_{23}$	2D ($E_{\text{obs}}^\mu, \cos\theta_{\text{obs}}^\mu$)	13.03
	3D ($E_{\text{obs}}^\mu, \cos\theta_{\text{obs}}^\mu, E_{\text{had}}'$)	11.25
Δm_{32}^2	2D ($E_{\text{obs}}^\mu, \cos\theta_{\text{obs}}^\mu$)	4
	3D ($E_{\text{obs}}^\mu, \cos\theta_{\text{obs}}^\mu, E_{\text{had}}'$)	2.57

True hierarchy	$\Delta\chi^2_{\text{ICAL-MH}}$ for 500 kton year exposure
NH	5.21
	8.50
IH	4.76
	8.13

~63% improvement from 2D to 3D (NH)
~71% improvement from 2D to 3D (IH)

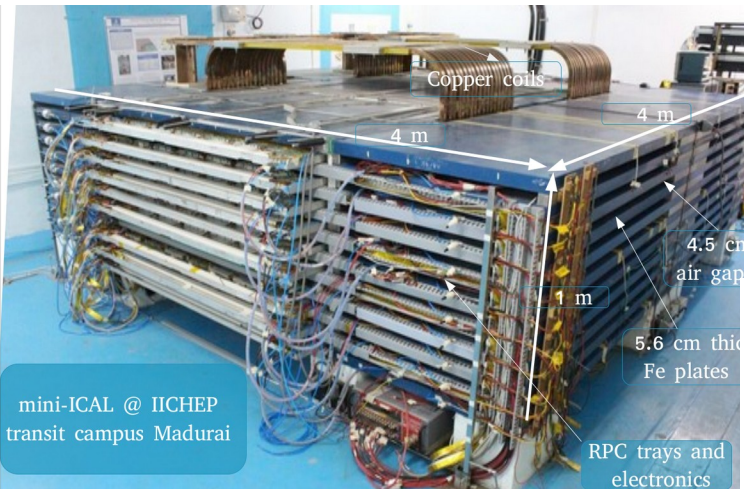
Other prospects for oscillation only physics

- › Sensitivity to ν_e events – with current geometry and also with a possible modified geometry.
- › 2–3 oscillation sensitivity from rock muons
- › Indirect sensitivities to oscillations from ν_τ events.
- › Dip and oscillation valley
- › Vacuum oscillations vs matter oscillations
- › Earth tomography

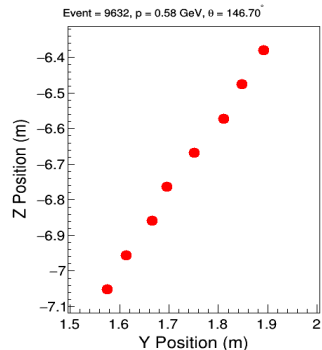
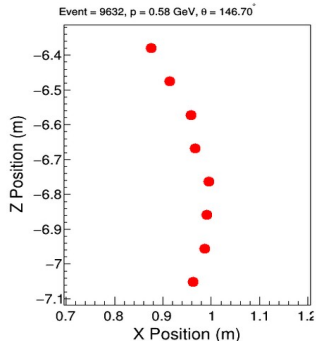
Sensitivity to new physics at ICAL

- Some of the new physics scenarios that can be studied at ICAL
 - Invisible decay of neutrinos
 - Non-standard interactions
 - Long-range forces
 - Sterile neutrinos
 - Galactic diffuse dark matter
 - Magnetic monopoles

Current status – mini ICAL

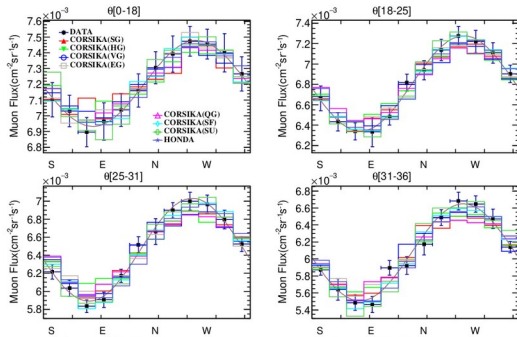


Operating since 2018 in IICHEP transit campus Madurai.



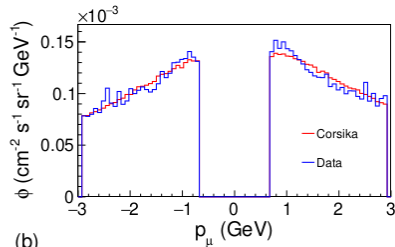
I = 900 A, B = 1.4 tesla

Measurements done at IICHEP transit campus, Madurai



Surface muon flux for different (θ , φ) bins with RPC only stack. East-West asymmetry observed.

S. Pethuraj, PhD thesis



(b)

Momentum spectra of cosmic ray muons

Validation of Kalma-filter technique too.

Apoorva Bhatt Dipak, PhD thesis

INO graduate training program

- Started in 2008
- Students work on ICAL or TINTIN the proposed NDBD experiment in INO
- 11 batches till now ~ 30 PhDs awarded

Contact and other details

India-based Neutrino Observatory

Home About us CoVID-19 FAQ People Career Notices World Scientists for INO Vidyay Samagam Online Lecture Series

Follow Us on

CoVID-19

INO in CoVID-19 Times

mini-ICAL

About mini-ICAL

Research Activities

INO-ICAL Physics White Paper

PhD Theses

NEWS

INO in times of CoVID-19: Click here

DAE of India and DOE of USA to cooperate for Neutrino Physics, Discovery Science, Accelerator and Particle Detector R&D: Copy of Agreement

Statement on INO from the three Indian entities

News updates

Statement of support for INO on home page of Indian Academy of Sciences (10-Dec-2019)

Welcome to INO!

<https://www.ino.tifr.res.in/ino/>

For some general neutrino & INO related talks please see <https://www.youtube.com/c/INOProject>



Thank you!

References

- 1) Pramana 88 (2017) 5, 79
- 2) 2014 JINST 9 P07001
- 3) JINST 8 (2013) P11003
- 4) JINST 9 (2014) 09, T09003
- 5) JINST 13 (2018) 03, C03006
- 6) JHEP 1410, 189 (2014)
- 7) EPJ C 77 (2017) 1, 54
- 8) <https://www.ino.tifr.res.in/ino/inoTheses.php>

Backup

The parameters in vacuum are modified in matter.

$$\Delta_{21}^m = \frac{1.27\Delta m_{32}^2 L}{E} \frac{1}{2} \left[\frac{\sin 2\theta_{13}}{\sin 2\theta_{13}^m} - 1 - \frac{A_{CC}}{\Delta m_{32}^2} \right],$$

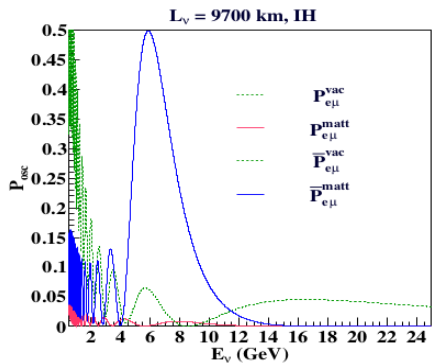
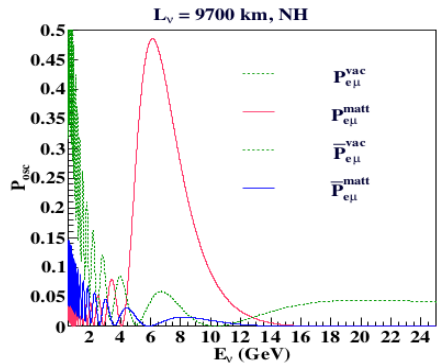
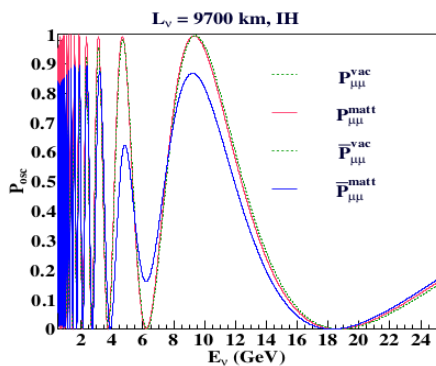
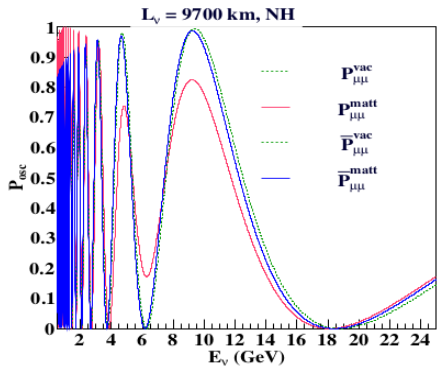
$$\Delta_{32}^m = \frac{1.27\Delta m_{32}^2 L}{E} \frac{1}{2} \left[\frac{\sin 2\theta_{13}}{\sin 2\theta_{13}^m} + 1 + \frac{A_{CC}}{\Delta m_{32}^2} \right], \quad (9)$$

$$\sin 2\theta_{12}^m \approx \frac{\sin 2\theta_{12}}{\left[(\cos 2\theta_{12} - (A_{CC}/\Delta m_{21}^2) \cos^2 \theta_{13})^2 + \sin^2 2\theta_{12} \right]^{1/2}} \quad (10)$$

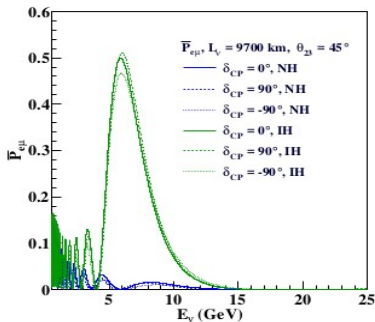
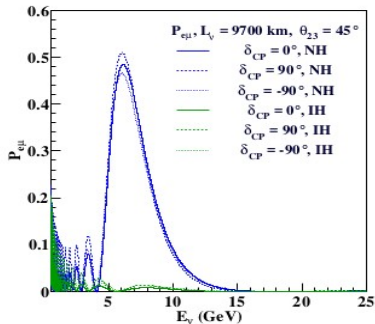
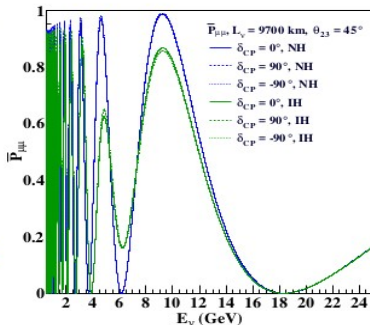
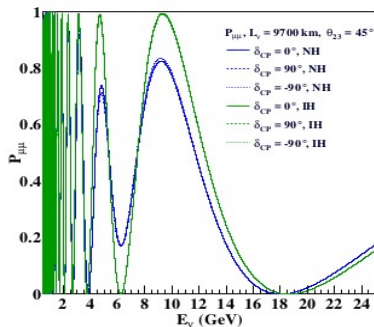
$$\Delta_{31}^m = \frac{1.27\Delta m_{32}^2 L}{E} \left[\frac{\sin 2\theta_{13}}{\sin 2\theta_{13}^m} \right] \quad (11)$$

$$\sin 2\theta_{13}^m = \frac{\sin 2\theta_{13}}{\left[(\cos 2\theta_{13} - (A_{CC}/\Delta m_{32}^2))^2 + \sin^2 2\theta_{13} \right]^{1/2}} \quad (12)$$

- E = neutrino energy, L = distance travelled by the neutrino.
- $A_{CC} = 2\sqrt{2}G_F N_e E$ is the matter potential; $A_{CC} \rightarrow -A_{CC}$ for $\bar{\nu}$.



Measurement of hierarchy independent of δ_{CP}



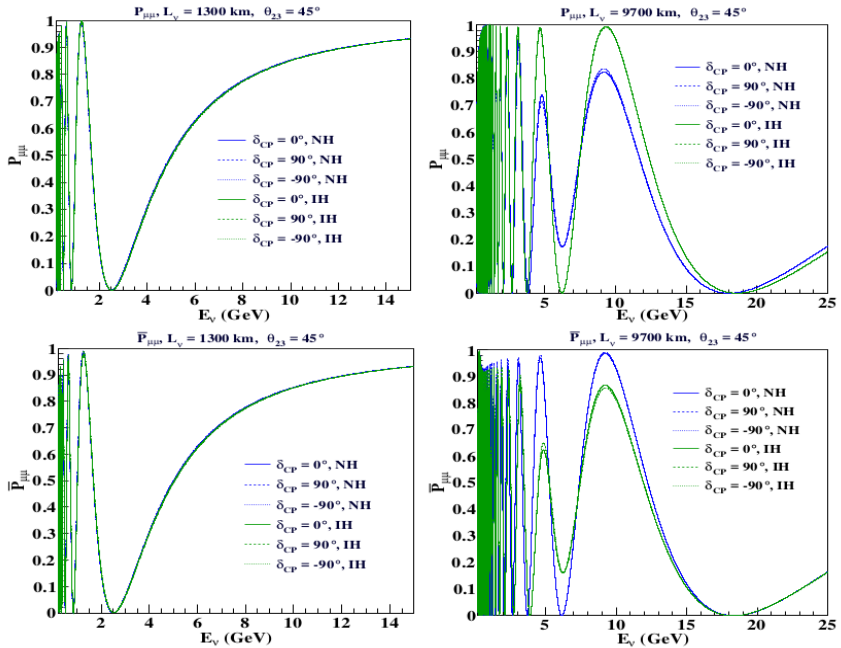


Figure 5: $\nu_\mu \rightarrow \nu_\mu$ and $\bar{\nu}_\mu \rightarrow \bar{\nu}_\mu$ for $L = 1300$ km (left) and 9700 km.

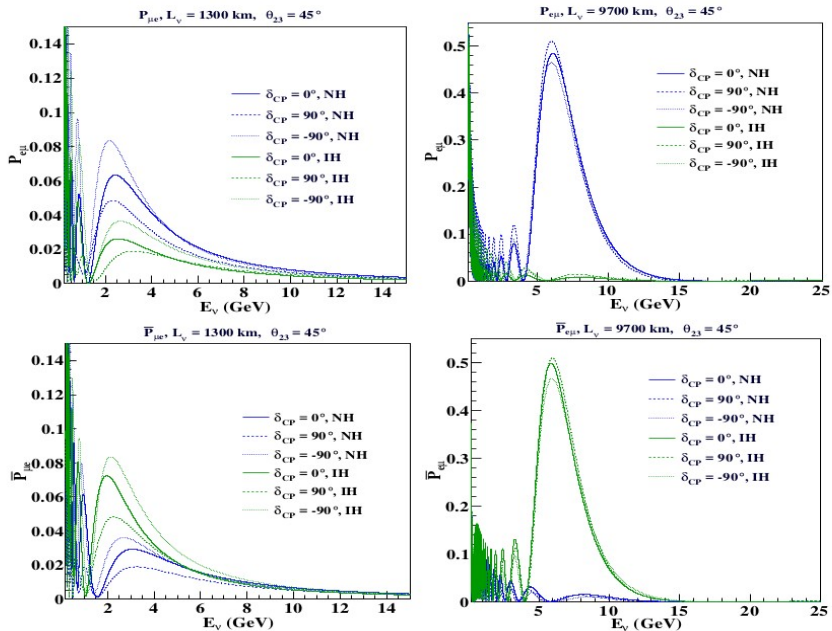
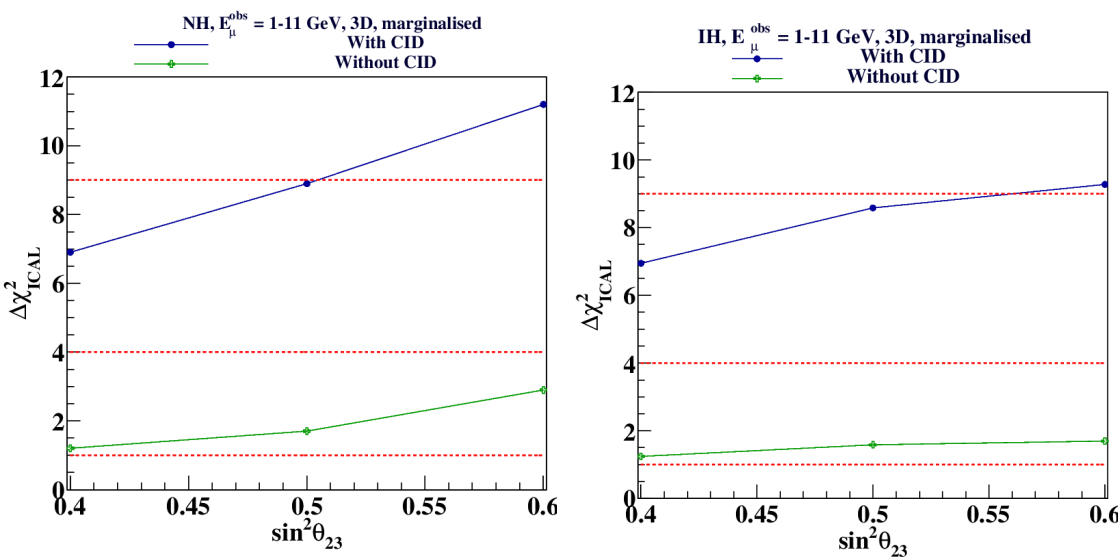


Figure 6: $\nu_\mu \rightarrow \nu_e$ and $\bar{\nu}_\mu \rightarrow \bar{\nu}_e$ for $L = 1300 \text{ km}$ (left) and $\nu_e \rightarrow \nu_\mu$ and $\bar{\nu}_e \rightarrow \bar{\nu}_\mu$ for $L = 9700 \text{ km}$.



Sensitivity to neutrino mass hierarchy with 500 kton year exposure of a magnetised iron detector with and without cid, for (left) true NH and (right) true IH and with marginalisation. Parameters taken as in JHEP 1410, 189 (2014) [arXiv: 1406.3689 [hep-ph]].

Orientation matrix method

Orientation Matrix Method (OMM). This method requires information on the reconstructed muon vertex. The hits in the X - and Y - planes are combined to form sets of 3-dimensional hits labelled (x, y, z) and the timing information is discarded. However, it is used to determine the muon vertex. For a collection of unit vectors $(x_i, y_i, z_i), i = 1, 2, 3 \dots, N$, the symmetric orientation matrix \mathbb{T} is defined as ref. [6]:

$$\mathbb{T} = \begin{pmatrix} \sum_{i=1}^N x_i^2 & \sum_{i=1}^N x_i y_i & \sum_{i=1}^N x_i z_i \\ \sum_{i=1}^N x_i y_i & \sum_{i=1}^N y_i^2 & \sum_{i=1}^N y_i z_i \\ \sum_{i=1}^N x_i z_i & \sum_{i=1}^N y_i z_i & \sum_{i=1}^N z_i^2 \end{pmatrix}. \quad (2.1)$$

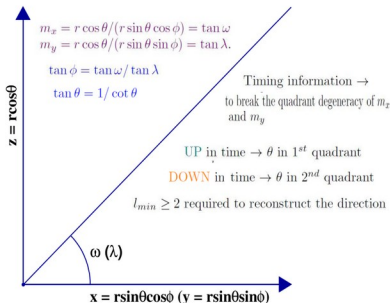
The eigen analysis of this symmetric matrix gives an idea of the shape of the underlying distribution. If a unit mass is assumed to be placed at each point, then the moment of inertia tensor of N points about any arbitrary axis $(x_{arb}, y_{arb}, z_{arb})$ is:

$$N - \begin{pmatrix} x_{arb} & y_{arb} & z_{arb} \end{pmatrix} \mathbb{T} \begin{pmatrix} x_{arb} & y_{arb} & z_{arb} \end{pmatrix}^T \quad (2.2)$$

Variation of the moment of inertia tensor gives information about the scatter of the points as the choice of axis varies. The axis about which the moment is least is the principal axis and is defined to be the shower direction. The MIGRAD and SIMPLEX minimizer algorithms, inbuilt in the TMinuit class in ROOT [7], were used for this calculation.

Raw hit method

- Average x and y positions in the i^{th} layer of an event are found separately.
- Hits within a time window of ≤ 50 ns within a layer are averaged.



$$N_{\mu^-} = N_{\mu^-}^0 \times P_{\mu\mu} + N_{e^-}^0 \times P_{e\mu},$$

$$N_{\mu^+} = N_{\mu^+}^0 \times \bar{P}_{\mu\mu} + N_{e^+}^0 \times \bar{P}_{e\mu},$$

$$N_{\mu^-}^{\text{tot}}(E_{\mu}^{\text{obs}}, \cos\theta_{\mu}^{\text{obs}}) = N_{\mu^-} \epsilon_{\text{rec}} \epsilon_{\text{cid}} + N_{\mu^+} \epsilon_{\text{rec}} (1 - \epsilon_{\text{cid}}),$$

$$N_{\mu^+}^{\text{tot}}(E_{\mu}^{\text{obs}}, \cos\theta_{\mu}^{\text{obs}}) = N_{\mu^+} \epsilon_{\text{rec}} \epsilon_{\text{cid}} + N_{\mu^-} \epsilon_{\text{rec}} (1 - \epsilon_{\text{cid}}),$$

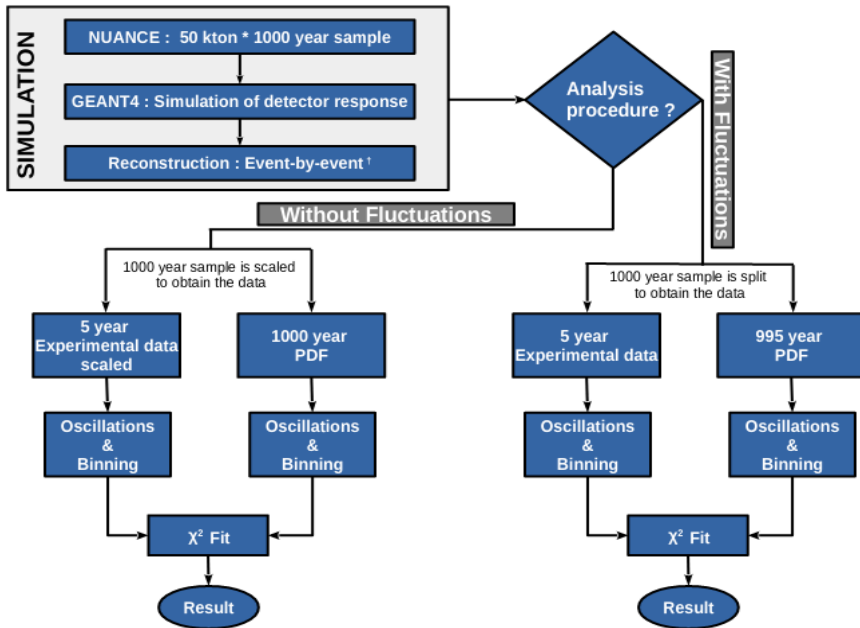
Table 2 Bins of the three observables, muon energy and direction and hadron energy, used in the analysis

Observable	Range	Bin width	No. of bins
E_{μ}^{obs} (GeV) (15 bins)	[0.5, 4]	0.5	7
	[4, 7]	1	3
	[7, 11]	4	1
	[11, 12.5]	1.5	1
	[12.5, 15]	2.5	1
	[15, 25]	5	2
$\cos\theta_{\mu}^{\text{obs}}$ (21 bins)	[-1.0, 0.0]	0.2	5
	[0.0, 0.4]	0.10	4
	[0.4, 1.0]	0.05	12
$E_{\text{had}}^{\text{obs}}$ (GeV) (4 bins)	[0, 2]	1	2
	[2, 4]	2	1
	[4, 15]	11	1

A more realistic analysis – Reconstruct events propagated through GEANT4 and use them for oscillation analysis.

Item	Criterion	Region	Events	Nomenclature
CS	$\chi^2/\text{ndf} < 10$	all	all	CS - χ^2 selection HS - Horizontal selection ZS - Z vertex selection NS - Nhits selection OS - Other selection CR - Central region PR - Peripheral region SR - Side region FC - Fully contained PC - Partially contained
HS	$ \cos \theta_z \geq 0.35$	all	all	
ZS	$z_v < 6$ m	all	up going	
	$z_v > -6$ m	all	down going	
NS	$N_{\text{hits}} > 0$	CR	all	
		PR	FC	
		SR	FC	
	$N_{\text{hits}} > 15$	PR	PC	
		SR	PC	
OS	$E_{\mu}^{\text{rec}} \geq 0.2$ GeV $E_{\mu}^{\text{rec}} \leq 50$ GeV $ \cos \theta_z^{\text{rec}} < 0.9999$ $ \phi_{\text{rec}} \geq 0.07$ rad	all	all	

Selection cuts applied to improve reconstruction. Cuts affect the statistics. Sample without cuts (WOS) and sample with cuts (WS) are used for oscillation analyses.



PhD thesis Rebin Raj

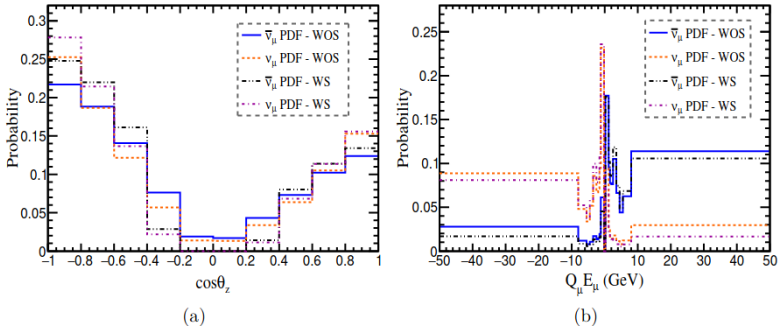


Figure 5.7: PDF for $\bar{\nu}_\mu$ and ν_μ are shown for (a) binning in $\cos\theta_z$, and (b) binning in E_μ . The $\bar{\nu}_\mu$ (ν_μ) entries for $q_\mu E_\mu < 0$ (> 0) indicate the charge misidentified content. The effect of the event selection is also shown by the distributions with (WS) and without (WOS) event selection criterion.

Observable	Range	Bin width	Bins	Total bins
E_μ (GeV)	$[-1.2, -0.2], [0.2, 1.2]$	1.0	2	18
	$[-2, -1.2], [1.2, 2]$	0.4	4	
	$[-2.5, -2], [2, 2.5]$	0.5	2	
	$[-5.5, -2.5], [2.5, 5.5]$	1.0	6	
	$[-8, -5.5], [5.5, 8]$	2.5	2	
	$[-50, -8], [8, 50]$	42	2	
$\cos\theta_z$	$[-1, 1]$	0.2	10	10

Table 5.3: The binning scheme for the reconstructed observables $\cos\theta_z$ and E_μ

$$\chi^2 = \min_{\{\xi_k\}} \sum_{i=1}^{n_{\cos\theta_z}} \sum_{j=1}^{n_{E\mu}} 2 \left[\left(N_{ij}^{\text{pdf}} - N_{ij}^{\text{data}} \right) - N_{ij}^{\text{data}} \ln \left(\frac{N_{ij}^{\text{pdf}}}{N_{ij}^{\text{data}}} \right) \right] + \sum_{k=1}^2 \xi_k^2,$$

$$N_{ij}^{\text{pdf}} = R \left[f T_{ij}^{\bar{\nu}} + (1 - f) T_{ij}^{\nu} \right] \left[1 + \sum_{k=1}^2 \pi_{ij}^k \xi_k \right].$$

$T_{ij}^{\bar{\nu}}$ and T_{ij}^{ν} are the normalized $\bar{\nu}$ and ν PDFs respectively

R = normalization factor in the fit which scales the PDF to the data entries.

The free parameter f describes the relative fraction of $\bar{\nu}_\mu$ and ν_μ in the sample.

250 kton year exposure

